J Cancer Res Clin Oncol (2018) 144:75–87
https://doi.org/10.1007/s00432-017-2541-0

ORIGINAL ARTICLE – CANCER RESEARCH

Molecular alterations in a new cell line (KU-Lu-MPPt3) established from a human lung adenocarcinoma with a micropapillary pattern

Yukiko Matsuo[1] · Kazu Shiomi[1] · Dai Sonoda[1] · Masashi Mikubo[1] · Masahito Naito[1] · Yoshio Matsui[1] · Tsutomu Yoshida[2] · Yukitoshi Satoh[1]

Received: 25 January 2017 / Accepted: 24 October 2017 / Published online: 1 November 2017

Abstract
Purpose Lung adenocarcinomas with a micropapillary pattern (MPP) are characterized by more frequent and pronounced vascular invasion, higher incidence and more advanced lymph node involvement and poorer prognosis than papillary adenocarcinomas without an MPP. Here we established a new lung cancer cell line featuring micropapillary structure.
Methods A 73-year-old never-smoker Japanese female, presenting with an abnormal chest shadow, was diagnosed with a clinical T2aN0M0 Stage IB lung adenocarcinoma and underwent left upper lobectomy with mediastinal lymph node dissection. Pathological study demonstrated a T2aN2M0 Stage IIIA micropapillary adenocarcinoma. Tumor cells were obtained from freshly resected lung material and used to establish the KU-Lu-MPPt3 cell line.
Results The KU-Lu-MPPt3 cells featured adherent monolayers, adherent tufts, and suspended tufts without adhesion under the same culture conditions. The cells were positive for cytokeratin, epithelial cell-adhesion molecules, E-cadherin, mucin-1, thyroid transcription factor-1, vimentin, and anti-programmed death ligand 1. Xenograft tumors clearly demonstrated micropapillary structures. Sequencing and fragment analysis of the epidermal growth factor receptor in the primary tumor tissue and KU-Lu-MPPt3 cells revealed an in-frame deletion E746-A750 in exon 19.
Conclusions This cell line represents a new model system for molecular studies of lung adenocarcinoma which may be suitable for investigation of cancer spread and also for development of molecular-targeting and immunotherapies, both in vitro and in vivo.

Keywords Cell line · Lung adenocarcinoma · Micropapillary · Molecular · Papillary

Abbreviations

AC-MPP	Adenocarcinoma with MPP
ALK	Anaplastic lymphoma kinase
ATS	American Thoracic Society
EDTA	Ethylenediaminetetraacetic acid
EGFR	Epidermal growth factor receptor
EML4	Echinoderm microtubule-associated protein-like 4
ERS	European Respiratory Society
FCS	Fetal calf serum
IASLC	International Association for the Study of Lung Cancer
IHC	Immunohistochemistry
ISCN	International System for Human Cytogenetic Nomenclature
JCRB	Japanese Collection of Research Bioresources
KRAS	Kirsten Ras
KU-Lu-MPPt3	Established cell line
MPP	Micropapillary pattern
N-2 supplement	Serum-free hormone supplement
NOD/SCID	Nonobese diabetic/severe combined immunodeficiency

Electronic supplementary material The online version of this article (https://doi.org/10.1007/s00432-017-2541-0) contains supplementary material, which is available to authorized users.

✉ Yukitoshi Satoh
ysatoh@med.kitasato-u.ac.jp

[1] Department of Thoracic Surgery, Kitasato University School of Medicine, 1-15-1 Kitasato, Minami-Ku, Sagamihara, Kanagawa 252-0374, Japan

[2] Department of Pathology, Kitasato University School of Medicine, 1-15-1 Kitasato, Minami-Ku, Sagamihara, Kanagawa 252-0374, Japan

NSCLC	Non-small cell lung cancer
PBS	Phosphate-buffered saline
PCR	Polymerase chain reaction
PD-1	Programmed death receptor 1
PD-L1	Programmed death ligand 1
RPMI	Roswell Park Memorial Institute
STR	Short tandem repeat
STAS	(Tumor) spread through air spaces
3D	Three-dimensional
TKI	Tyrosine kinase inhibitor
TTF-1	Thyroid transcription factor-1

Introduction

Lung cancer is the leading cause of malignancy-related death worldwide, including in Japan (Torre et al. 2015; Committee for Scientific Affairs, The Japanese Association for Thoracic Surgery 2014). Recent progress in molecular understanding has revealed that lung cancer is very heterogeneous in terms of driver oncogenes and hence the response to different drugs (Swanton and Govindan 2016). The incidence of particular molecular alterations of a given driver oncogene is dependent on various factors, such as ethnicity, sex, and age of the patient. For example, mutation of the epidermal growth factor receptor (*EGFR*) gene are frequently observed in patients who are female, non-smoking, and with East Asian ethnicity (Swanton and Govindan 2016; Mitsudomi 2014; Yatabe et al. 2015). Targeted therapy for these lung cancers has been established based on evidence regarding mainly common mutations; that is, exon 19 deletions and L858R (Mitsudomi 2014).

In 2015, the International Association for the Study of Lung Cancer (IASLC)/American Thoracic Society (ATS)/European Respiratory Society (ERS) published a revised classification for lung tumors, in which a micropapillary-predominant subtype was newly added to adenocarcinomas (Travis et al. 2015). The adenocarcinoma with a micropapillary pattern (AC-MPP), with MPP areas varying in amount from only minor to predominant, accounts for a substantial percentage of tumors, characterized by more frequent and prominent vascular invasion, a higher incidence and more advanced lymph node involvement, and a poorer prognosis than conventional papillary adenocarcinomas without an MPP (Amin et al. 2002; Miyoshi et al. 2003; Satoh et al. 2009; Maeda et al. 2009). The MPP is now believed to predispose to lymphatic and venous invasion (Nakashima et al. 2015). A possible explanation for this is loss of cell polarity (Luna-Moré et al. 1994). Tumor budding in lung cancer may reflect, in part, an epithelial–mesenchymal transition phenotype (Yamaguchi et al. 2010; Aokage et al. 2011). Therefore, the cell lines established from the AC-MPP should be useful for researching metastatic mechanisms. It is now widely recognized that non-small cell lung cancer (NSCLC) cell lines are useful as preclinical models for evaluating targeted therapies and for investigating resistance to therapy. Many cell lines harboring *EGFR* mutations have been reported (Engelman et al. 2007; Paez et al. 2004). Because genomic changes, especially for driver mutations, are stable, such properties are generally maintained in long cultured cell lines (Gazdar et al. 2016). However, additional *EGFR*-mutated cell lines are needed as tools for basic research to develop novel therapeutic strategies for AC-MPP. In 1999, a micropapillary invasive breast cancer cell line was established by fine-needle aspiration from a patient (Araujo et al. 1999). Many NSCLC cell lines had been reported in the literature. However, to our knowledge, there has been no report on establishment of any AC-MPP cell line derived from lung malignancy.

Most recently, immunotherapy has added important advances in the treatment of advanced NSCLC and has become a new standard of second-line care (Araujo et al. 1999; Tsao et al. 2016). However, we have yet to obtain effective predictive biomarkers to identify good responders and long-term survivors (Tsao et al. 2016).

In the present study, we established a new cell line derived from a patient with AC-MPP harboring an *EGFR* mutation and featuring focal programmed death ligand 1 (PD-L1) expression as revealed immunohistochemically. This cell line should be useful for investigating the biological characteristics of AC-MPP.

Materials and methods

Ethics statement

The present investigation was carried out according to the Declaration of Helsinki, and was approved by the ethics committee of Kitasato University Medical Ethics Organization (Approval No. KME B09-33). The patient previously agreed to participate in the study and gave written informed consent.

Patient

A 73-year-old Japanese female, never-smoker, presented with an abnormal chest shadow. She was diagnosed as having a left lung adenocarcinoma of clinical T2aN0M0 Stage IB. She underwent a left upper lobectomy with mediastinal lymph node dissection. Pathological study demonstrated a T2aN2M0 Stage IIIA micropapillary adenocarcinoma. After surgery, she was treated with three courses of adjuvant chemotherapy consisting of cisplatin and vinorelbine. However, recurrence in the ipsilateral lung and bones occurred 1 year after surgery. Her Eastern Cooperative Oncology Group

performance status was 1. Because her tumor cells harbored *EGFR* mutation, she received EGFR-tyrosine kinase inhibitor (TKI) therapy and remains in stable condition.

Establishment of the micropapillary adenocarcinoma cell line

Tumor cells were isolated from resected lung tissue using the following method and procedures. Tissue samples were washed with phosphate-buffered saline (PBS) (Life Technologies; Osaka, Japan), and then moistened with a little amount of culture medium, Roswell Park Memorial Institute (RPMI) 1640 (Sigma-Aldrich; Tokyo, Japan) supplemented with 10% fetal calf serum (FCS) (Biowest; San Diego, CA, USA), serum-free hormone supplement (N-2 supplement) (Life Technologies), 2 mM L-glutamine, 100 U/mL of penicillin, 100 µg/mL of streptomycin (Life Technologies), and 10 µg/mL of gentamicin (Life Technologies) on culture dishes. After mincing with surgical scissors, fragments were plated onto collagen-I coated 35-mm dishes (Iwaki; Tokyo, Japan) with 3 mL of culture medium at 37 °C in 5% CO_2/95% air. After overnight incubation, medium containing floating cells were collected from all original dishes. Collected cells were washed with PBS, and those that were dead were removed using a ClioCell Pro Kit (ClioCell; London, UK). Viable cells were plated on new collagen-I coated dishes until the medium turned yellow. Fibroblasts were removed carefully with a cell scraper several times. When a cancerous cell colony attained the ability to propagate profusely, it was picked up with a pipette tips, avoiding fibroblasts, and immediately plated on a new dish. At the time of confluence, adherent cells were subcultured with 0.25% trypsin–ethylenediaminetetraacetic acid (EDTA) (Life Technologies). A subcultivation ratio of 1:3–1:5 proved appropriate. For authentication, we delegated short tandem repeat (STR) assays and mycoplasma contamination tests to the Japanese Collection of Research Bioresources (JCRB) Cell Bank (http://cellbank.nibiohn.go.jp/english/).

Chromosome analysis by quinacrine banding

We delegated karyotype assays to the Fukuyama Medical Laboratory Co. Ltd. (Fukuyama, Japan). The cultures were harvested and chromosome analysis was performed by quinacrine banding. The subsequent karyotype description followed the recommendations of the ISCN (2013).

In vitro growth and morphology

To observe morphology in a three-dimensional (3D) environment, suspended and adherent cells were harvested and plated on NenoCulture Dishes (Organogenix, Inc; Kawasaki, Japan). Then, to confirm viability and dynamic states of cells, aliquots (2×10^5) were plated on collagen-I coated 35-mm dishes in triplicate for each time point on days 2, 4, and 8. The number of viable cells was counted for each type, in suspension and adherent.

Culture medium

The optimal culture medium condition for cell proliferation was determined by comparison of the supplementation of the RPMI 1640 basal medium with serum (10% FCS), N-2 supplement, and both of them together (10% FCS and N-2 supplement). Only viable adherent cells (1×10^5) were plated on collagen-I coated 35-mm dishes in 9–10 plated wells in each medium. Both suspended and adherent cells were counted at days 2, 4, and 8 of culture. Those in suspension were harvested by pipette, whereas adherent examples were harvested with 0.25% trypsin–EDTA (Life Technologies).

Population-doubling time

To determine population-doubling time, numbers of viable cells were determined daily for 8 and 12 days, in experiments 1 and 2, respectively. Only viable adherent cells (1×10^5) were plated on collagen-I coated 35-mm dishes in triplicate for each time point. FCS supplemented in culture medium used was manufactured by Biowest for experiment 1 and by Corning (New York, USA) for experiment 2. Suspended and adherent cells were counted separately, and the doubling time was calculated from the exponential growth phase using the following formula: $\log 2(t - t_0)/\log N - \log N_0$.

Xenografts in immunodeficient mice

All animal studies were performed in accordance with protocols approved by the Kitasato University School of Medicine Animal Care Committee. Non-obese diabetic/severe combined immunodeficiency (NOD/SCID) mice at 8 weeks of age were purchased from CLEA (Tokyo, Japan) and housed in a specific pathogen-free environment and allowed free access to food and water. Cultured adherent cells ($5–10 \times 10^6$/side) were injected subcutaneously, bilaterally into the backs of the mice. The right side cells were suspended in 50 µL of PBS mixed with 50 µL of Corning® Matrigel® (Corning), and the left side cells were suspended in 100 µL of PBS. After 30–36 days, samples from the tumors were fixed in 10% buffered formalin and processed for embedding in paraffin and then serial sectioning at 4-µm. Sections were stained with hematoxylin and eosin and mounted on slides to analyze morphology and by immunohistochemistry for assessment of cytokeratin, thyroid transcription factor-1 (TTF-1), and PD-L1 expression.

Table 1 Antibodies used

Antibody	Supplier	Dilution	pH	Pretreatment
Vimentin	Dako	1:200	6	Autoclave
N-cadherin	Dako	1:50	9	Autoclave
E-cadherin	Dako	1:50	9	Microwave
Muc-1	Leica	1:50	9	Microwave
TTF-1	Leica	1:100	6	Autoclave
Cytokeratin	Nichirei	Undiluted	Protease	Not treated
Ep-cam	Cell Marque	1:100	6	Autoclave
PD-L1(SP263)	Ventana	1:1	6	Autoclave

Table 2 Primers used for direct sequencing and fragment analysis of EGFR mutations

Exon18	Forward	5′-GCTCCCAACCAAGCTCTC-3′
	Reverse	5′-CCCAAACACTCAGTGAAACA-3′
Exon19	Forward	5′-ATTGCCAGTTAACGTCTTCCT-3′
	Reverse	5′-GGTGGGCCTGAGGTTCAGA-3′
Exon20	Forward	5′-GAAACTCAAGATCGCATTCATGC-3′
	Reverse	5′-GCAAACTCTTGCTATCCCAGGAG-3′
Exon21	Forward	5′-AGGGCATGAACTACTTGGA-3′
	Reverse	5′-AAATGCTGGCTGACCTAAAG-3′

Immunohistochemistry

For immunohistochemical analysis, suspended and adherent cells were collected separately and introduced into iPGell (Genostuff; Tokyo, Japan), fixed with 10% buffered formalin and processed for embedding in paraffin. Sections cut at 4-μm were deparaffinized and rehydrated. Antigens were retrieved by heat-mediated or enzymatic digestion (Table 1). Endogenous peroxidase activity was quenched by incubation with 3% H_2O_2 in water for 10 min, and then nonspecific staining was quenched by incubation with protein block (DAKO; Tokyo, Japan) for 10 min. Specimens were incubated with primary antibodies appropriately diluted in buffer (DAKO) (Table 1) for 2 h at room temperature. After subsequent incubation with a ChemMate Envision Kit/HRP (DAKO) for 30 min, binding in all specimens was visualized with diaminobenzidine.

EGFR mutation analysis

Genomic DNA was isolated from fresh cultured cells and fragments of snap-frozen primary tumor tissue using a QIAamp DNA Mini Kit (Qiagen; Venlo, Netherlands), Exons 18 through 21 of *EGFR* were analyzed by polymerase chain reaction (PCR) direct sequencing. Exon 19 deletion mutations were also confirmed by fragment analysis (Table 2). Both analyses were performed on an autosequencer (3500 Dx Genetic Analyzer, Applied Biosystems; Waltham, MA, USA). To detect exon 18 mutations (G719X), exon 20 mutations (T790M), and exon 21 mutations (L858R and L861Q), the Cycleave method was used based on the basic principle of real-time PCR (StepOnePlus™; Applied Biosystems) (Table 3).

Statistical analysis

We compared continuous variables among the groups using Steel–Dwass multiple comparison tests. P values < 0.05 were considered significant in all experiments. Data are expressed as mean ± SEM.

Results

Establishment of the KU-Lu-MPPt3 cell line and morphologic characteristics in vitro

Two weeks to 1 month after initiating the primary culture, cancer cells were propagated and formed colonies with raised edges and also formed tufty aggregates. After reseeding and passage three or four times, we selected the cell line

Table 3 Primers used for cycleave analysis of *EGFR* mutations

Exon18	G719 Wild, G719A	Forward	5′-CATGTCTGGCACTGCTTTC-3′
		Reverse	5′-CCAGGGACCTTACCTTATACAC-3′
	G719C, G719S	Forward	5′-GCTGAGGTGACCCTTGTCT-3′
		Reverse	5′-TGCCAGGGACCTTACCTTAT-3′
Exon20	T790M	Forward	5′-TGCGAAGCCACACTGAC-3′
		Reverse	5′-TCTGCACACACCAGTTGA-3′
Exon21	L858R	Forward	5′-GCAGCATGTCAAGATCAC-3′
		Reverse	5′-TGACCTAAAGCCACCTC-3′
	L861Q	Forward	5′-TTCCCATGATGATCTGTCC-3′
		Reverse	5′-GCTGACCTAAAGCCACCTC-3′

demonstrating most appropriate proliferation. Maintained in subculture and passaged 32 times. The cell line had three unique different morphologic features: adherent monolayers, adherent tufts or suspended tufts without adhesion under the same culture conditions (Fig. 1). In the 3D environment, the cells formed spheroids and were found suspended without adhesion. Spheroids showed botryoidal and spherical shapes (Fig. 1d), and could be successfully subcultured. The same morphology was observed using ultralow attachment dishes or medium containing polymer gels for 3D cell culture (data not shown). Multiple cells adhered to the bottom of dishes and increased gradually over time when only suspended cells were plated on collagen-I coated dishes. The ability to re-adhere was observed for 8.76% of the total cell counts at day 2, 16.7% at day 4, and 47.4% at day 8 (Fig. 2). We designated the new cell line as KU-Lu-MPPt3.

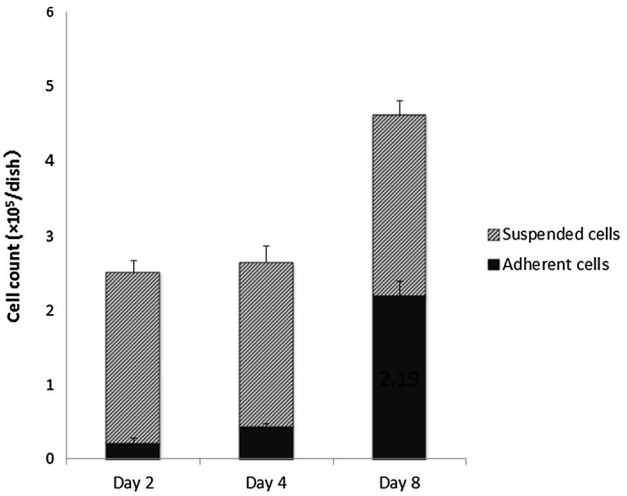

Fig. 2 Time-dependent morphological changes in culture. Only viable cells in suspension (2×10^5) were plated on dishes, and the counts of adherent and suspended cells were conducted separately at days 2, 4, and 8 of culture. Each bar indicates a mean ± SEM. The ordinate shows the number of total cells ($n = 3$ for each group)

Authentication and mycoplasma contamination testing

KU-Lu-MPPt3 cells and extracted genomic DNA from snap-frozen primary tumor tissue were sent to the JCRB Cell Bank for authentication and mycoplasma contamination

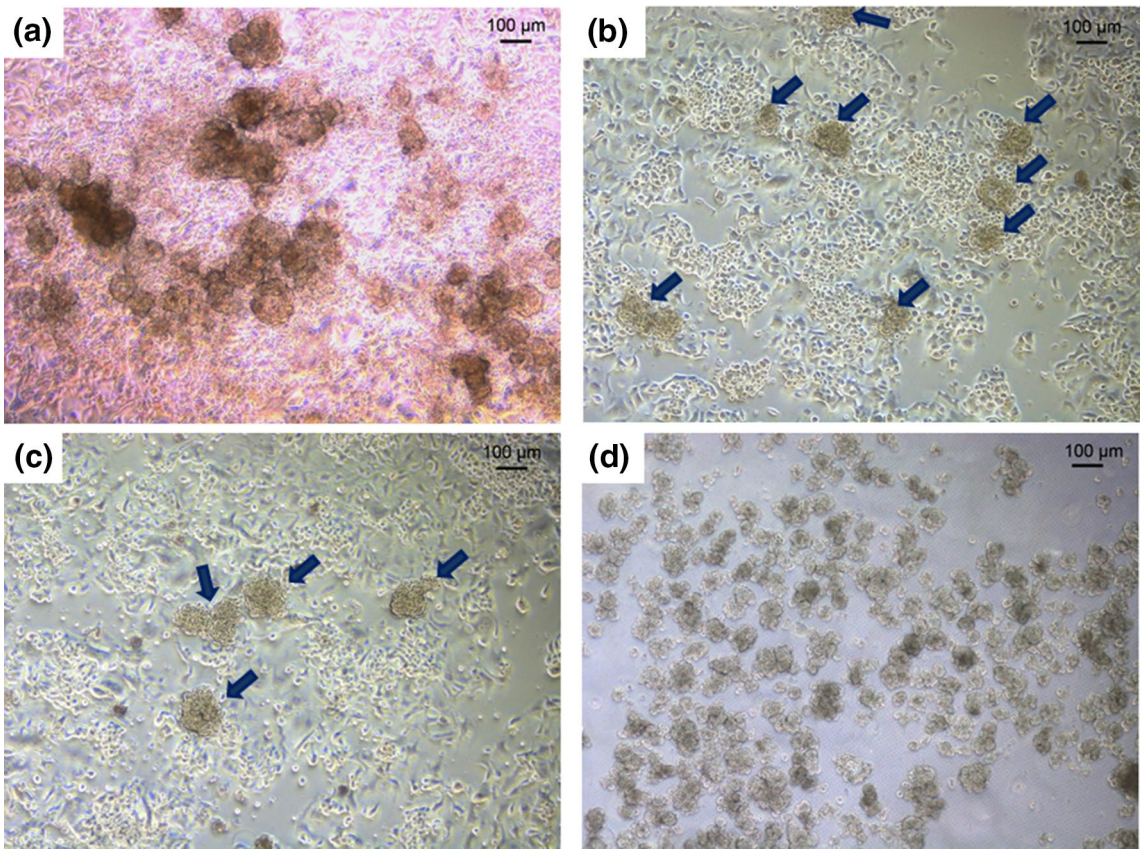

Fig. 1 Morphologic findings for KU-Lu-MPPt3 cells. **a** Primary culture adherent monolayer cells and tufty aggregates of cells with rising edges at day 25 (×10). **b** The established cell line featuring adherent monolayer cells and adherent tufts (arrows) (×5). **c** Suspended tufts without adherence (arrows) (×5). **d** Spheroids showed botryoidal and spherical shapes without adherence (×5)

testing. The results showed that cell line to be of human origin with the same DNA profile as donor tissue using polymorphic STR. Mycoplasma was not detected using a MycoAlert™ Mycoplasma Detection Kit (Lonza, Basel, Switzerland).

Culture medium condition and growth curve

To evaluate the effect of culture medium condition on KU-Lu-MPPt3 proliferation, suspension and adherent populations were counted sequentially. The most efficient condition was RPMI 1640 with 10% FCS in combination with the N-2 supplement at day 8 (Fig. 3). Similar tendencies were observed at days 2 and 4 (data not shown). The doubling times in experiments 1 and 2 were 74.5 h (Fig. 4a) and 59.2 h (Fig. 4b). Increase in counts between adherent and suspension cells was divergent.

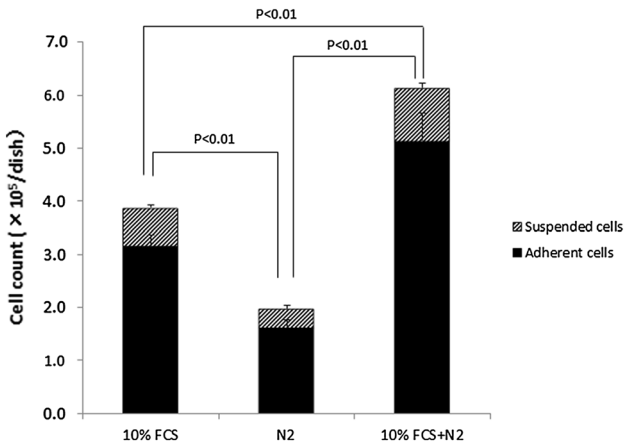

Fig. 3 Effects of supplements to RPMI 1640 basal medium on cell proliferation. Established cells were counted separately for adherent populations and those in suspension after day 8 of culture. Each bar indicates a mean ± SEM. The ordinate shows the number of total cells ($n = 9$ or 10 for each group)

Immunohistochemistry

Immunohistochemical analysis for protein expression of KU-Lu-MPPt3 showed the same patterns of protein expression as primary tumor tissue (Fig. 5a). No differences were evident among adherent, suspension, or 3D environment cells (Fig. 5b, c), all being positive for cytokeratin, Ep-CAM (epithelial cell-adhesion molecule), E-cadherin, mucin-1, and TTF-1. Vimentin showed partially positive results, while N-cadherin was negative (Fig. 5).

Karyotype analysis

Characterizations of complex chromosomal abnormalities in the cell line KU-Lu-MPPt3 were showed by quinacrine banding analysis as follows (Fig. 6):

66~71<4n>,XXXX,-3,-5,-5,add(5)(p15)x2,-6,-8,-8,add(8)(p2?),i(8)(q10),-9,-9,-10,-10,add(11)(p15)x2,-12,-12,-13,-13,add(14)(p11.2)x2,-15,-15,add(15)(p13)x2,-17,-17,-18,-18,-19,-19,-20,-20,-20,-20,-22,-22,+mar1x2+mar2,+mar3,+1~5mar[cp10].

Tumorigenicity in mice

Implanted tumor cells slowly grew in subcutaneous sites in mice. Figure 7 shows a tumor at 30 days after injection. The clearly demonstrated micropapillary structures with air spaces (Fig. 7). Immunohistochemically, cytokeratin, and

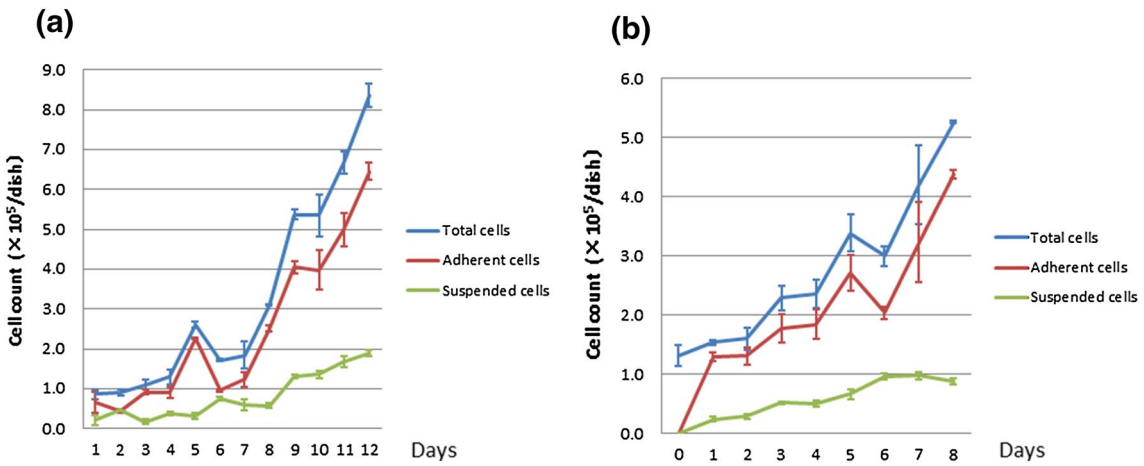

Fig. 4 Cell growth curve in vitro. Only viable adherent cells (1×10^5) were plated on dishes, and counts of adherent and suspended cells were conducted separately at intervals of 24 h. In experiments 1 and 2, we used different sources of fetal calf serum (FCS). **a** Experiment 1 for 12 days. The doubling time of total cells was 74.5 h. **b** Experiment 2 for 8 days. The doubling time was 59.2 h ($n = 3$ for each day)

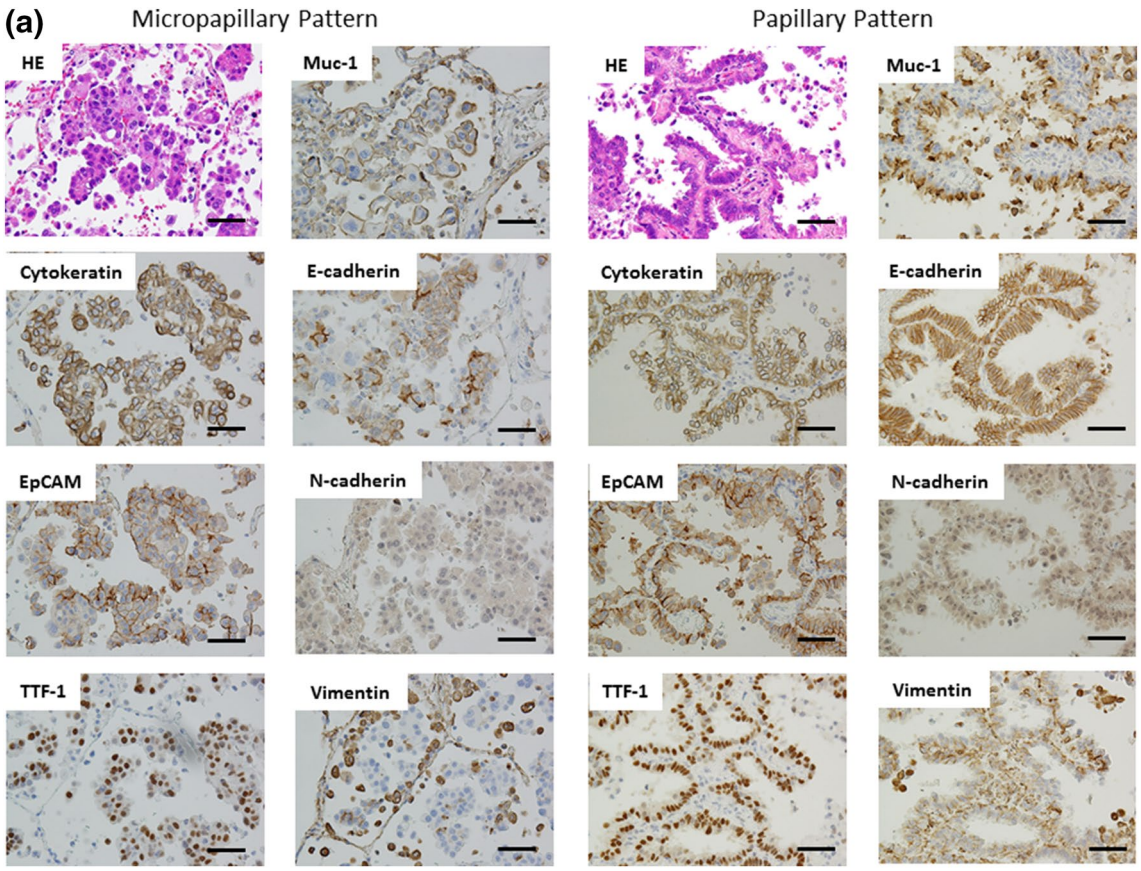

Fig. 5 **a** H&E and immunohistochemical staining of primary tumor tissue (×20). **b** H&E staining and immunohistochemical staining of the established cell line (×20). Adherent and suspended cells showed the same results. **c** H&E and immunohistochemical staining of the cell line in the 3D environment (×20) (each bar = 50 μm)

TTF-1 were positive in the excised tumor (Fig. 8). Therefore, the samples were determined to be AC-MPP. Moreover, anti-PD-L1 was partially positive (Fig. 8).

EGFR mutation

Sequencing and fragment analysis of *EGFR* revealed an exon 19 mutation, an in-frame deletion E746-A750 (Fig. 9), in both the KU-Lu-MPPt3 cells and the primary lung tumor tissue. Both the wild type and the mutation type peaks in the cell line showed almost the same levels of signals. In contrast, since the primary tumor contained normal tissue, the wild type peak of was greater than its mutation peak (data not shown).

Discussion

To our knowledge, this is the first report of establishment of a cell line from AC-MPP tissue. In general, serum-free medium such as serum-free defined medium (ACL-4) is used to enhance the capacity for cancer cell growth (Brower et al. 1986; Masuda et al. 1991). However, a cell line from AC-MPP has not yet been established by conventional methods. Instead of ACL-4, we applied an N-2 supplement and succeeded in generating a new AC-MPP cell line (Seo et al. 2013).

Lung adenocarcinoma with MPP, newly classified in the IASLC/ATS/ERS classification, have particular molecular characteristics, including *EGFR* mutations, expression of echinoderm microtubule-associated protein-like 4 (EML4) and alteration of anaplastic lymphoma kinase (*ALK*) fusion or other driver oncogenes (Travis et al. 2015; Furukawa et al. 2016; Inamura et al. 2010). Detailed pathologic examination has shown significant genotype–phenotype correlations between *EGFR* mutations and presence of a micropapillary pattern (Inamura et al. 2010; Ninomiya et al. 2009). Although accumulating data support the concept of AC-MPP being an adverse prognostic indicator, little is currently known about the factors and mechanisms conferring a more aggressive nature on this tumor type (Nakashima et al. 2015).

Our KU-Lu-MPPt3 lung cancer cell line established from lung tumor tissue of a Japanese female patient with AC-MPP

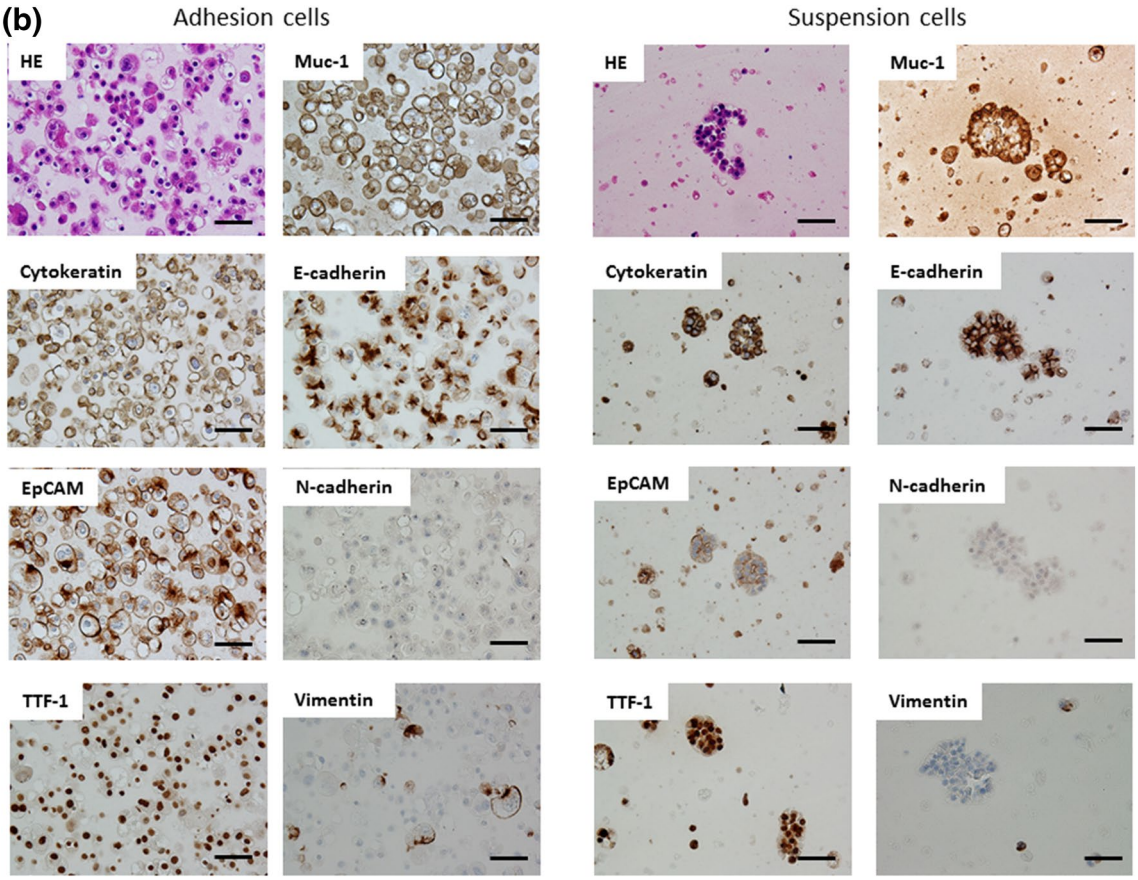

Fig. 5 (continued)

showed partially positive results for vimentin. Recently, we demonstrated that vimentin expression is prevalent and markedly up-regulated in AC-MPP, which might reflect the essential biological feature of poorer differentiation or dedifferentiation of MPP, and this might have a role in the acquisition and increase of invasiveness and consequently a more malignant nature (Nakashima et al. 2015).

Moreover, the cell line also harbored the E746-A750 *EGFR* in-frame deletion in exon 19. We could also successfully establish an NOD/SCID mouse model bearing xenografts of KU-Lu-MPPt3 cells. The recurrent tumor in our original lung cancer patient after adjuvant chemotherapy initially responded very well to EGFR-TKI treatment. Recently we showed that the hobnail cell type and AC-MPP and lepidic lung adenocarcinomas are associated with a high incidence of *EGFR* mutations (Ninomiya et al. 2009). AC-MPP frequently feature a *EML4-ALK* fusion gene and *EGFR* mutations (Furukawa et al. 2016). For example, 46.4% of 28 adenocarcinomas diagnosed with AC-MPP harbored mutually exclusive mutations: 32.1% in *EGFR*, 3.6% in Kirsten Ras (*KRAS*), and 10.7% in *EML4-ALK* fusion genes. For comparison, lung adenocarcinomas without MPP harbored 30.4% *EGFR* mutations, 12.3% *KRAS* mutations, 2.2% *EML4-ALK* fusion genes and 0.7% *PIK3CA* mutations (Furukawa et al. 2016). Therefore, it is suggested that the molecular pathogenesis of AC-MPP may be somewhat different from that of other adenocarcinomas.

Consequently, we believe that the KU-Lu-MPPt3 cell line is of value in understanding the mechanisms underpinning EGFR-TKI therapy in particular. The in-frame deletion E746-A750 in exon 19 means that it could be a useful tool to investigate acquired resistance to EGFR-TKI and we are currently planning to establish an EGFR-TKI-resistant variant.

Recently, Kadota et al. (2015) indicated that presence of tumor spread through air spaces (STAS) is a significant risk factor for recurrence in small lung adenocarcinomas treated with limited resection. Their results also indicated a strong association between the presence of STAS and adverse pathologic features. Furthermore, STAS was more frequently identified in cases that had a micropapillary

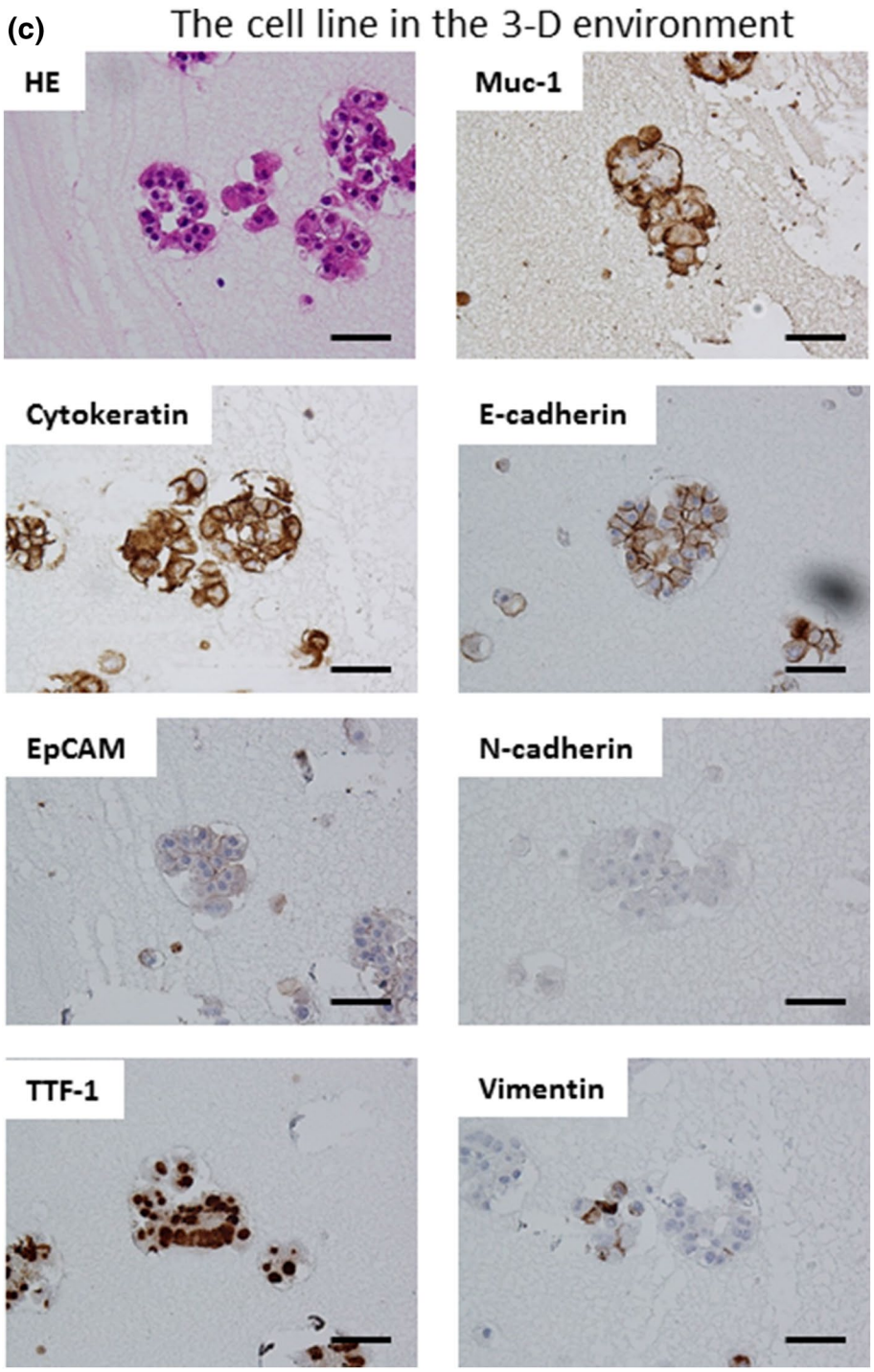

Fig. 5 (continued)

pattern in the main tumor (Kadota et al. 2015). The morphology of AC-MPP is unique regarding its floating of cells in alveolar spaces. In the present study, we observed multiple cells in suspension that had derived from AC-MPP adhering to the bottom of dishes (Fig. 10). Moreover, suspended cells were to some extent independent of adhering cell components, because increase in counts was divergent between adherent and suspension cells and the growth curve of the latter showed a gradual rise. Therefore, we strongly believe that KU-Lu-MPPt3 should be a useful

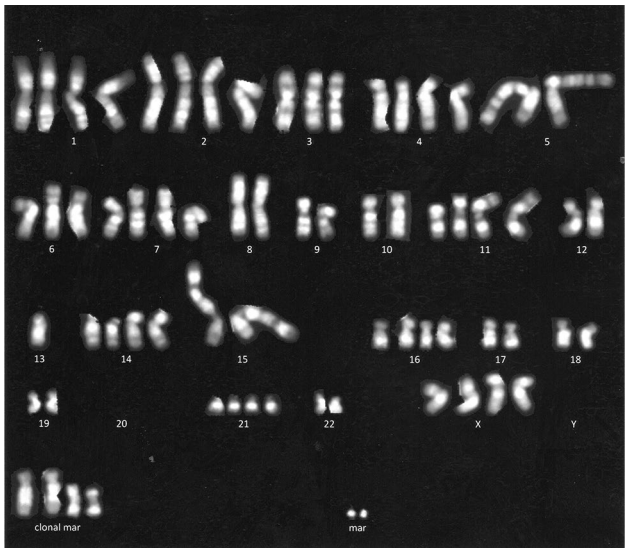

Fig. 6 Image of chromosome analysis by quinacrine banding. Representative karyotype analysis of 10 KU-Lu-MPPt3 cells. Note chromosomal aberrations on many chromosomes except chromosome X, 1, 2, 4, 7, 16 and 21

model for investigating the biological characteristics of STAS and tumor islands (Kadota et al. 2015; Morales-Oyarvide and Mino-Kenudson 2016).

Activation of the immune system to treat cancer has long been a target and recently the tide has undoubtedly changed. Namely, immunotherapy with antibodies to prevent interaction of the PD-L1 with the programmed death receptor 1 (PD-1) has dramatically improved the survival of some patients with advanced lung cancer (Araujo et al. 1999). Although additional insights into the predictors of response to PD-1/PD-L1 inhibition have been gained through the study of melanomas, we could not find any predictors, to date, for lung cancer (Tsao et al. 2016; Kerr et al. 2015). Therefore, performance of translational studies to optimize predictive biomarkers, such as PD-L1 expression or others obtained through DNA and/or RNA sequencing is a high priority. The fact that the KU-Lu-MPPt3 cell line partially showed a positive reaction to PD-L1 immunohistochemically (IHC), calls into question the value of PD-L1 IHC as a predictive biomarker to select a patient subgroup for therapy.

In conclusion, we have established an AC-MPP-derived cell line, KU-Lu-MPPt3, which provides a new model system for further studies of lung adenocarcinoma. Hopefully it will prove suitable for investigation of cancer spread and also for exploration of efficacious chemotherapeutic approaches, molecular-targeted therapy, and immunotherapy both in vivo and in vitro. This cell line has now been

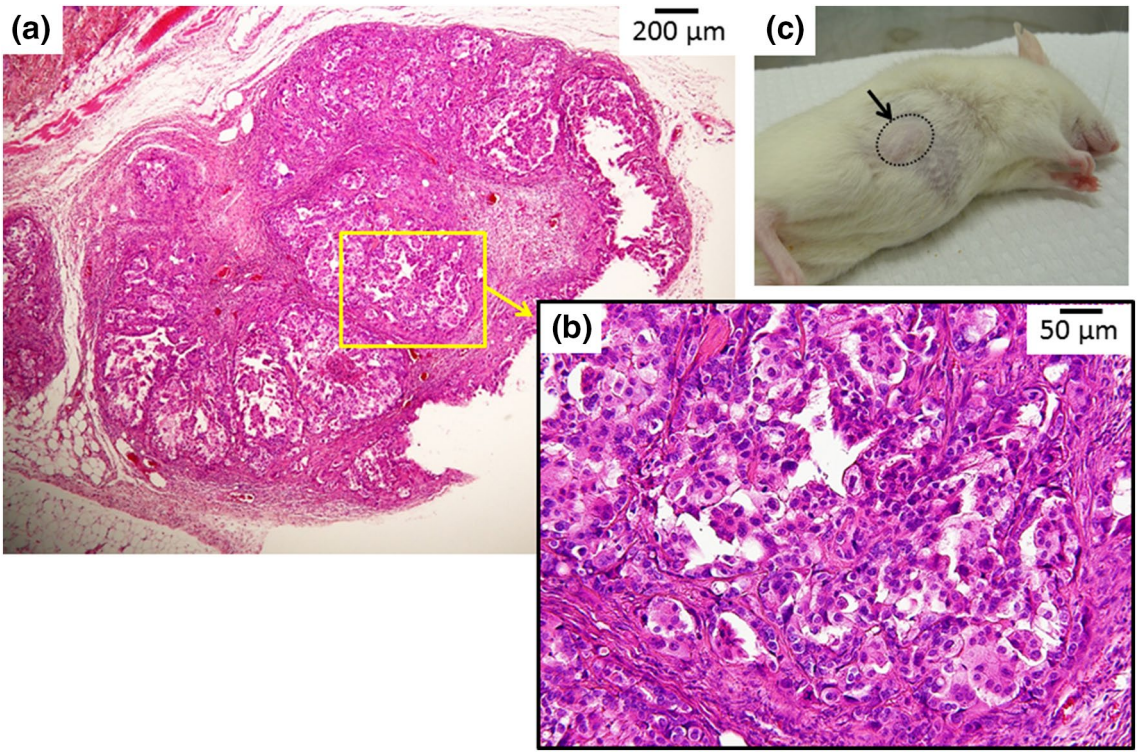

Fig. 7 Tumorigenicity in mouse subcutaneous tissue. **a** Microscopic images of H&E staining of an excised tumor specimen from a mouse. Note the papillary structure with partial MPP within airspaces; **b** High-power field; **c** the xenograft in the mouse

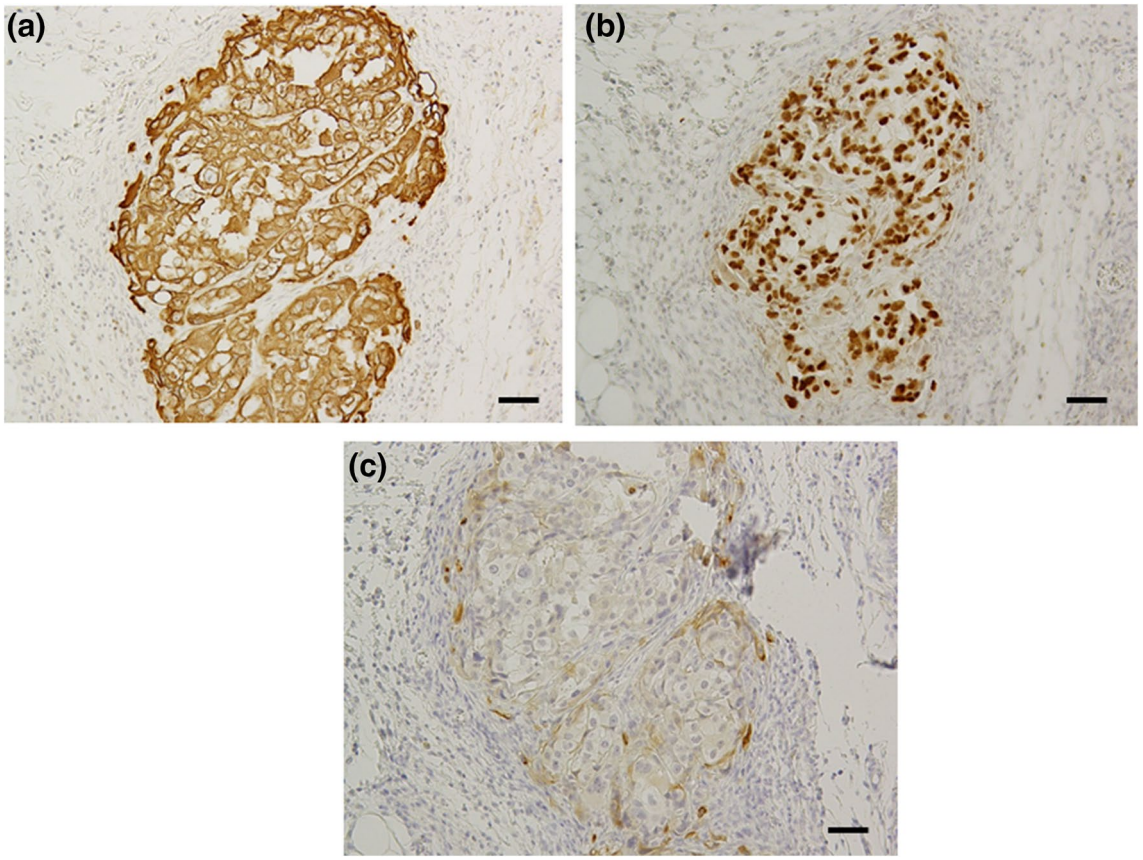

Fig. 8 Immunohistochemical staining for cytokeratin (**a**), TTF-1 (**b**) and anti-PD-L1 (**c**) in implanted cells (each bar = 50 µm)

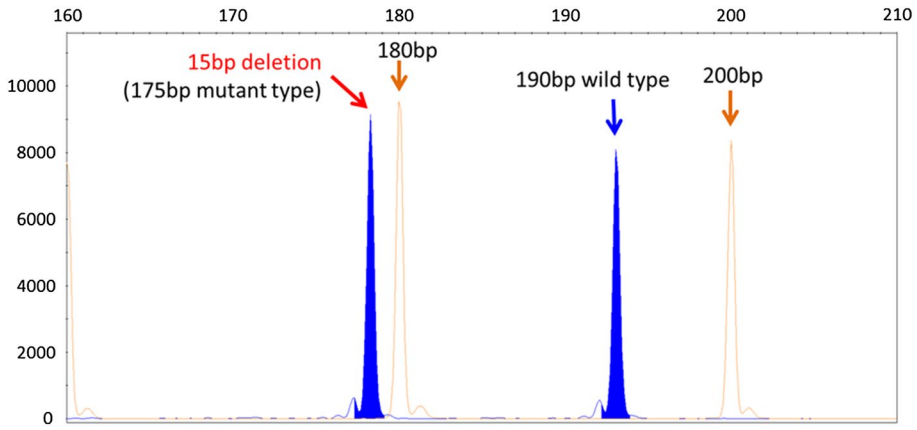

Fig. 9 EGFR exon 19 fragment analysis. Double peaks were detected. The right peak is the wild type, and the left is the mutant type. Both 180 and 200 bp are standard peaks

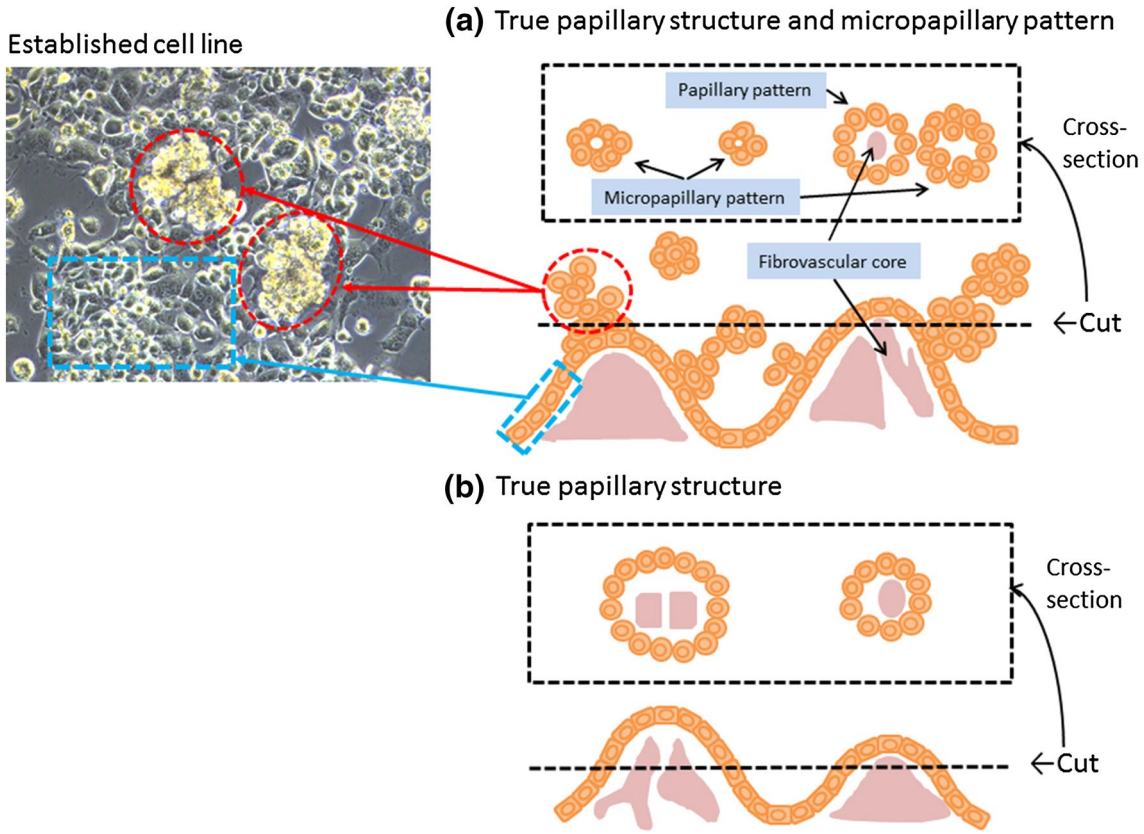

Fig. 10 Schema of the morphology of lung adenocarcinoma with and without a micropapillary pattern and the new cell line with unique structures

deposited to the JCRB Cell Bank where it is widely available to the scientific community.

Acknowledgements This work was supported by Japan Society for the Promotion of Science (JSPS) KAKENHI Grant nos. 24592099 and 26461896. We thank Dr. Koji Eshima, Department of Immunology, Kitasato University School of Medicine, and Dr. Jiang SX, Division of Pathology, Toshiba Rinkan Hospital, for their technical assistance.

Compliance with ethical standards

Conflict of interest The authors have no conflicts of interest to disclose.

Ethical approval This study was approved by the ethics committee of Kitasato University Medical Ethics Organization (Approval No. KME B09-33)

References

Amin MB, Tamboli P, Merchant SH et al (2002) Micropapillary component in lung adenocarcinoma: a distinctive histologic feature with possible prognostic significance. Am J Surg Pathol 26:358–364

Aokage K, Ishii G, Ohtaki Y et al (2011) Dynamic molecular changes associated with epithelial–mesenchymal transition and subsequent mesenchymal–epithelial transition in the early phase of metastatic tumor formation. Int J Cancer 128:1585–1595

Araujo RW, Paiva V, Gartner F et al (1999) Fine needle aspiration as a tool to establish primary human breast cancer cultures in vitro. Acta Cytol 43:985–990

Brower M, Carney DN, Oie HK et al (1986) Growth of cell lines and clinical specimens of human non-small cell lung cancer in a serum-free defined medium. Cancer Res 46:798–806

Committee for Scientific Affairs, The Japanese Association for Thoracic Surgery, Masuda M, Okumura M, Doki Y et al (2014) Thoracic and cardiovascular surgery in Japan during 2014. Annual report by The Japanese Association for Thoracic Surgery. Gen Thorac Cardiovasc Surg 64:665

Engelman JA, Zejnullahu K, Mitsudomi T et al (2007) MET amplification leads to gefitinib resistance in lung cancer by activating ERBB3 signaling. Science 316:1039–1043

Furukawa M, Toyooka S, Ichimura K et al (2016) Genetic alterations in lung adenocarcinoma with a micropapillary component. Mol Clin Oncol 4:195–200

Gazdar AF, Hirsch FR, Minna JD (2016) From mice to men and back: an assessment of preclinical model systems for the study of lung cancers. J Thorac Oncol 11:287–299

Inamura K, Ninomiya H, Ishikawa Y et al (2010) Is the epidermal growth factor receptor status in lung cancers reflected in clinicopathologic features? Arch Pathol Lab Med 134:66–72

Kadota K, Nitadori J, Sima CS et al (2015) Tumor spread through air spaces is an important pattern of invasion and impacts the frequency and location of recurrences after limited resection for small stage I lung adenocarcinomas. J Thorac Oncol 10:806–814

Kerr KM, Tsao MS, Nicholson AG et al (2015) Programmed death-ligand 1 immunohistochemistry in lung cancer: in what state is this art? J Thorac Oncol 10:985–989

Luna-Moré S, Gonzalez B, Acedo C et al (1994) Invasive micropapillary carcinoma of the breast. A new special type of invasive mammary carcinoma. Pathol Res Pract 190:668–674

Maeda R, Isowa N, Onuma H et al (2009) Lung adenocarcinomas with micropapillary components. Gen Thorac Cardiovasc Surg 57:534–539

Masuda N, Fukuoka M, Takada M et al (1991) Establishment and characterization of 20 human non-small cell lung cancer cell lines in a serum-free defined medium (ACL-4). Chest 100:429–438

Mitsudomi T (2014) Molecular epidemiology of lung cancer and geographic variations with special reference to EGFR mutations. Transl Lung Cancer Res 3:205–211

Miyoshi T, Satoh Y, Okumura S et al (2003) Early-stage lung adenocarcinomas with a micropapillary pattern, a distinct pathologic marker for a significantly poor prognosis. Am J Surg Pathol 27:101–109

Morales-Oyarvide V, Mino-Kenudson M (2016) Tumor islands and spread through air spaces: distinct patterns of invasion in lung adenocarcinoma. Pathol Int 66:1–7

Nakashima H, Jiang SX, Sato Y et al (2015) Prevalent and up-regulated vimentin expression in micropapillary components of lung adenocarcinomas and its adverse prognostic significance. Pathol Int 65:183–192

Ninomiya H, Hiramatsu M, Inamura K et al (2009) Correlation between morphology and EGFR mutations in lung adenocarcinomas Significance of the micropapillary pattern and the hobnail cell type. Lung Cancer 63:235–240

Paez JG, Jänne PA, Lee JC et al (2004) EGFR mutations in lung cancer: correlation with clinical response to gefitinib therapy. Science 304:1497–1500

Satoh Y, Hoshi R, Horai T et al (2009) Association of cytologic micropapillary clusters in cytology samples with lymphatic spread in clinical stage I lung adenocarcinomas. Lung Cancer 64:277–281

Seo J, Park SJ, Kim J et al (2013) Effective method for the isolation and proliferation of primary lung cancer cells from patient lung tissues. Biotechnol Lett 35:1165–1174

Swanton C, Govindan R (2016) Clinical implications of genomic discoveries in lung cancer. N Engl J Med 374:1864–1873

Torre LA, Bray F, Siegel RL et al (2015) Global cancer statistics, 2012. CA Cancer J Clin 65:87–108

Travis WD, Brambilla E, Burke AP, Marx A, Nicholson AG (2015) WHO classification of tumours of the lung, pleura, thymus and heart, 4th edn. IARC Press, Lyon

Tsao AS, Scagliotti GV, Bunn PA Jr et al (2016) Scientific advances in lung cancer 2015. J Thorac Oncol 11:613–638

Yamaguchi Y, Ishii G, Kojima M et al (2010) Histopathologic features of the tumor budding in adenocarcinoma of the lung: tumor budding as an index to predict the potential aggressiveness. J Thorac Oncol 5:1361–1368

Yatabe Y, Kerr KM, Utomo A et al (2015) EGFR mutation testing practices within the Asia Pacific Region: results of a multicenter diagnostic survey. J Thorac Oncol 10:438–445